

Nanostructured silver octahedra co-modified with amine and aryl-anchored groups for synergistic surface-enhanced Raman spectroscopy

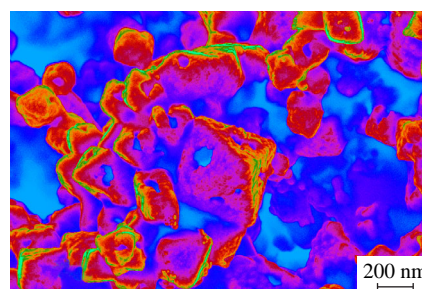
Anna A. Semenova^a and Eugene A. Goodilin^{*a,b}

^a Department of Materials Science, M. V. Lomonosov Moscow State University, 119991 Moscow, Russian Federation. E-mail: goodilin@yandex.ru

^b Department of Chemistry, M. V. Lomonosov Moscow State University, 119991 Moscow, Russian Federation

DOI: 10.1016/j.mencom.2022.11.014

Octahedral pseudomorphs of nanostructured silver co-modified with amine and aryl-anchored groups have been found to exhibit a synergistic effect in practical applications of surface-enhanced Raman spectroscopy due to a combination of enhanced chemical sorption and charge transfer effects for quinone analytes. This new approach allows combinatorial modification of the surface of SERS-active materials for selective capturing and detection of target analytes.



Keywords: silver, octahedra, nanostructuring, pseudomorphs, surface-enhanced Raman spectroscopy.

Silver nanostructured materials remain the bright leaders in highly sensitive non-invasive diagnostics for environmental monitoring and biomedical applications based on the fundamental phenomena of surface-enhanced Raman spectroscopy (SERS).^{1–5} In this context, silver mesocages are often considered as the most intriguing nanostructured objects,^{6–10} since their chemical formation pathways use shape-retaining transformations of suspensions of shaped precursor particles into metallic silver hydrosols.^{6–9} This mechanism leads to a local reconstruction of crystal lattices, a change in the phase volume and the development of a complex internal nanostructure. Thus, the appearance of such pseudomorphs ensures the predominance of a porous structure and an increase in the probability of creating a large number of ‘hot spots’ (narrow gaps between close nanoparticles inside pseudomorphs), which significantly enhance the SERS effect and also result either in an increased surface area for adsorption of target analytes, or in extended spectral sensitivity of pseudomorphs.^{5,8,9}

The main feature of octahedral pseudomorphs is the expected large number of hot spots, which provide a greater SERS enhancement compared to the possible influence of other factors, such as the shape or size of nanoparticles. In these terms, the size distribution definitely plays a minor role, since the size of the nanoparticles is in the range of several hundreds of nanometers. Purely spherical nanoparticles prepared by classical methods are often difficult to use due to their narrow and almost ‘fixed’ plasmon bands, located irrespective of most widely used Raman lasers, while shifting the laser wavelength closer to the plasmon resonance position by using anisotropic nanoparticles would be a complicated way in the presence of electrolytes that change the shape of the particles by recrystallization. In this context, pseudomorphs seem to be an appropriate choice for SERS measurements.

These unique features make their SERS applications of practical interest. In this work, we analyzed various conditions for the

formation of octahedral pseudomorphs of nanostructured silver and proposed their co-modification with amine and aryl-anchored groups to demonstrate a synergistic effect when using SERS in terms of combinatorial modification of the surface of SERS-active materials for selective capture and detection of target analytes.^{11–17}

We systematically investigated the influence of the prehistory of preparation on the morphology (Figure 1) and properties (Figures 2 and 3) of nanostructured silver pseudomorphs obtained by soft chemistry methods.^{†5,8,9} Obviously, only a narrow combination of silver nitrate concentrations, temperature, molecular weight of the polyvinylpyrrolidone (PVP) surfactant and its added amount leads to an advantageous morphology of hollow porous silver octahedra [Figure 1(a),(b)], consisting of subgrains with sizes of coherent scattering regions in the range of 19–22 nm according to XRD

[†] Six series of samples were prepared using an approach developed previously^{5,8,9} after a systematic modification of a known published method.⁶ The first stage included the formation of polyhedral silver(I) oxide/silver chloride particles by adding dropwise 0.5 M ammonia solution to an aqueous solution (50 ml) of silver(I) nitrate of various concentrations (10, 50 or 100 mM in series 1 and 100 mM in all other series) at 25 °C in the presence of solution of polyvinylpyrrolidone (PVP) as a specific facet-selective surfactant ($M = 1\,300\,000\text{ g mol}^{-1}$ in series 3 and $M = 40\,000\text{ g mol}^{-1}$ in all other series, the weight of added PVP was 0.5, 5 and 50 mg in series 2 and 3 and 0.5 mg in all other series). After that, a 2 M aqueous sodium hydroxide solution (3 ml) was added to the colorless solution with vigorous stirring to yield polyhedral Ag₂O particles. The resulting precipitate was washed several times with distilled water and ethanol. At the second stage, hydrogen peroxide (10%, 20 ml) was added to the precipitate with stirring as a reducing agent, followed by injection of etching 0.5 M ammonia solution (5, 10, 20 or 50 ml) in series 4. In series 5, the solution temperature was additionally raised to 40 or 60 °C. In special series 6, silver was precipitated from 10, 50 or 100 mM silver nitrate solutions as AgCl rather than Ag₂O. The synthesized silver particles were collected by centrifugation (4000 rpm, 10 min, Sartorius Sigma) and finally redispersed in ethanol. The target materials

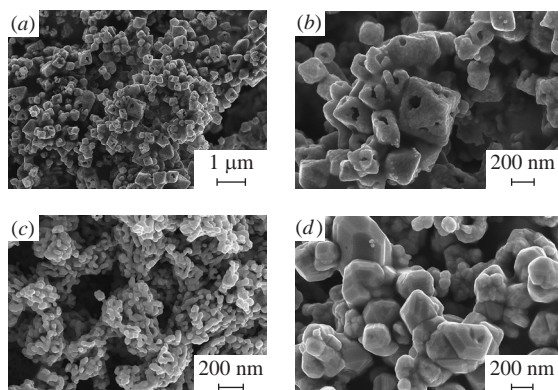


Figure 1 Typical SEM images of nanostructured silver samples with different morphologies due to their prehistory: (a) general view of octahedral pseudomorphs of nanostructured silver prepared using PVP and silver(I) oxide at room temperature (series 3, 0.5 mg of PVP), (b) details of the microstructure of such skeletons with etched holes and silver subgrains with ‘hot spots’, (c) the result of the application of silver chloride precursors (series 6) and (d) grain growth and faceting at higher temperatures of preparation in solutions (series 5, 60 °C).

data [Figure 2(a)].[‡] In some cases, the use of chlorides instead of Ag₂O precursors completely deteriorates the pseudomorphic morphology, but retains multiple contacts of silver nanoparticles [Figure 1(c)]. Higher temperatures produce dense recrystallized silver grains without interesting SERS features. Among the six series, numbering about 20 different samples with different prehistory of preparation and morphology, the samples of series 3 demonstrated the most acceptable peculiarities (see Figure 1).[†] These samples, but not only them, were used further to demonstrate their SERS activity. The samples consisted of pure cubic silver, demonstrating phase purity, like most of the others [see Figure 2(a)]. The nature of nanostucturing manifests itself in the presence of usually smooth plasmon resonance peaks⁹ [Figure 2(b)], which indicates the possibility of significantly efficient absorption of visual light radiation in a wide wavelength range.

As a result, silver octahedra [see Figure 1(a),(b)] exhibit a contact surface area clearly increased due to volume changes during reduction and etching reactions, a platonic shape resembling the appearance of silver(I) oxide precursor particles and are nanostructured bodies with multiple interparticle contacts, of which the final silver octahedra are built.

The SERS spectrum of the methylene blue dye^{11,12} (Figure 3),[§] measured using nanostructured silver octahedra, fully confirms the

were characterized using a Carl Zeiss NVision 40 field emission scanning electron microscope at an accelerating voltage of 0.5–5 kV. The most probable sequence of the described reactions could be given by the equations for the reduction ($\text{Ag}_2\text{O} + \text{H}_2\text{O}_2 = 2\text{Ag} + \text{O}_2 + \text{H}_2\text{O}$ and $2\text{AgCl} + \text{H}_2\text{O}_2 + 2\text{NaOH} = 2\text{Ag} + 2\text{NaCl} + \text{O}_2 + 2\text{H}_2\text{O}$) and etching ($\text{Ag}_2\text{O} + \text{H}_2\text{O} + 4\text{NH}_3 = 2[\text{Ag}(\text{NH}_3)_2]^+ + 2\text{OH}^-$, $\text{AgCl} + 2\text{NH}_4\text{OH} = [\text{Ag}(\text{NH}_3)_2]\text{Cl} + 2\text{H}_2\text{O}$ and $\text{Ag} + 1/4\text{O}_2 + 2\text{NH}_3 + 1/2\text{H}_2\text{O} = [\text{Ag}(\text{NH}_3)_2]^+ + \text{OH}^-$) of precipitates.

[‡] XRD data were obtained using a Rigaku D/MAX 2500 instrument with a rotating copper anode (CuK α radiation, graphite monochromator, 2θ range of 5–80°, 0.02° step). To estimate the coherent scattering regions (CSR) of octahedral particles, the Debye–Scherrer formula $d = K\lambda/(\beta\cos\theta)$ was used, where d is the CSR size, K is the Scherrer constant, taken for simplicity as 1, $\lambda = 1.5406 \text{ \AA}$, β is the XRD peak width at half height, and θ is the Bragg angle. The silicon standard was measured to subtract the instrumental broadening. UV-VIS absorption spectra were recorded using a Perkin–Elmer Lambda 950 UV-VIS spectrophotometer with a diffuse reflectance accessory attached. The measurements were carried out in the spectral range of 200–800 nm at a scanning rate of 2 nm s^{-1} .

[§] Raman and SERS spectra were measured using a Renishaw InVia Raman microscope equipped with 20 mW lasers emitting at 633 nm (see Figure 3) or 532 nm (Figure 4) and a power neutral density filter (10%). All spectra were collected using a 20 \times objective lens and a 10 s acquisition time. A silicon wafer was used for calibration.

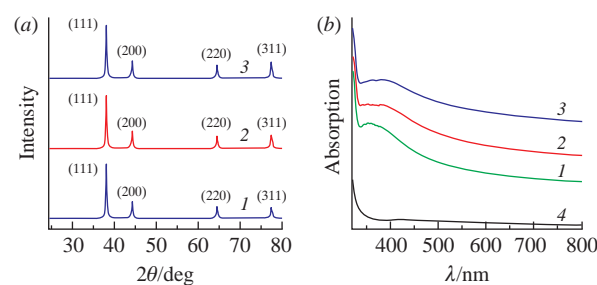
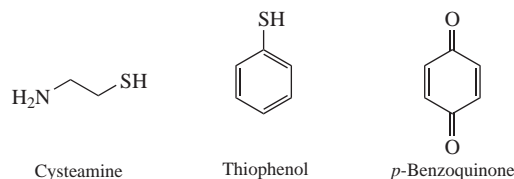


Figure 2 (a) XRD patterns and (b) UV-VIS absorption/diffuse scattering spectra of typical nanostructured silver samples (series 3) prepared with (1) 0.5, (2) 5 and (3) 50 mg of PVP. For comparison, the UV-VIS spectrum of (4) the glass substrate is shown.

high SERS activity of the resulting nanostructured pseudomorphic silver. The spectrum measured in the extended range makes it possible to clearly identify almost all known registered peaks of the methylene blue dye at its concentration below 0.1 μM . The enhancement coefficient can be estimated at least 10^6 if the high intensity of the measured spectrum is taken into account compared to normal Raman spectra (without silver octahedra) of other analytes such as cysteamine, thiophenol and *p*-benzoquinone (Figure 3, inset) showing only background signals at 1 mM concentration. This seems to be a severe model test for the prepared material, which has been successfully passed. It should be noted that the red laser used for excitation usually prevents the high luminescence of such a dye, so we excluded the use of a green laser and dyes of the rhodamine family (for the same reason). However, Figure 2(b) shows that the wavelength of the red laser does not fall into the maximum of the plasmon band, but into the light absorption shoulder; nevertheless, the discussed nanostructured silver material demonstrates its performance in a wide spectral range. An additional feature, according to our previous experience, never discussed in detail in the literature, is the presence of a special mode at *ca.* 200 cm^{-1} , observed exclusively for nanostructured silver and never found for bulk metallic silver.



Cysteamine and thiophenol show high affinity for the silver surface due to the presence of thiol groups, so both molecules are strong capping agents for silver octahedra. The molecules are fixed on the silver surface by strong Ag–S bonds. The formation of such bonds changes the vibrational modes of the molecules, since new bonds with silver, affecting either other bonds or the redistribution of electron density, potentially change the conformations of molecules. This usually results in slightly different positions and intensities of the SERS peaks compared to conventional Raman modes of the same substances. In addition, cysteamine will fold onto the silver with its amine group, and this bond is relatively weak, moreover, this particular molecule can be attached with both groups to the surface of silver, since it is flexible and not as rigid as thiophenol. As for quinone, its molecule is also rigid, and its fixation through oxygen on the surface of silver can be considered as more physical than chemical adsorption. At the same time, *p*-benzoquinone is an acceptor molecule that easily forms the well-known stable charge-transfer complex (CTC, quinhydrone) with aromatic donor hydroquinone (quinol), which is simultaneously stabilized by intramolecular OH–O hydrogen bonds. Previously, we proposed the use of specially designed pairs of donors and

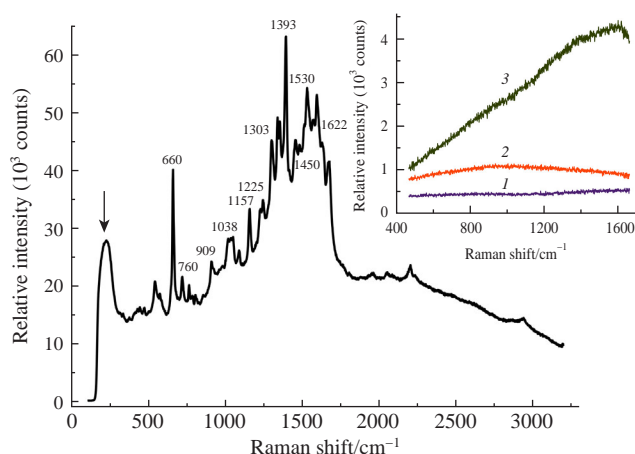


Figure 3 Typical extended range SERS spectrum of the methylene blue dye^{11,12} (concentration 0.1 μM) measured using nanostructured silver octahedra (series 2, 0.5 mg of PVP). The arrow marks the unusual ‘nanosilver’ mode, which is often observed in SERS-active samples. The inset shows the normal Raman spectra of (1) cysteamine, (2) thiophenol and (3) *p*-benzoquinone at a concentration of 1 mM.

acceptors¹⁸ to catch target molecules and enhance their SERS signals with initially low spectral amplification in SERS. Such a CTC would be possible between thiol and benzoquinone if the stability of the complex were sufficiently high. However, there are no hydroxyl groups in thiophenol and, therefore, it is impossible to glue the molecules closely by hydrogen bonds in order to provide donor–acceptor charge transfer. Conversely, cysteamine cannot provide CTC, but can catch quinone through hydrogen bonding to the amino group.

SERS of thiophenol (Figure 4, spectrum 2),[¶] as expected, exhibits a strong vibrational mode at 1576 cm^{-1} assigned¹³ to the symmetric C–C aromatic ring mode. At the same time, C–C–H and C–C–S bending (1108 cm^{-1}), C–C–C bending and C–S vibration (1071 cm^{-1}), as well as C–H ring bending (1031 cm^{-1}) modes decrease in intensity, probably due to strong Ag–S bonding.

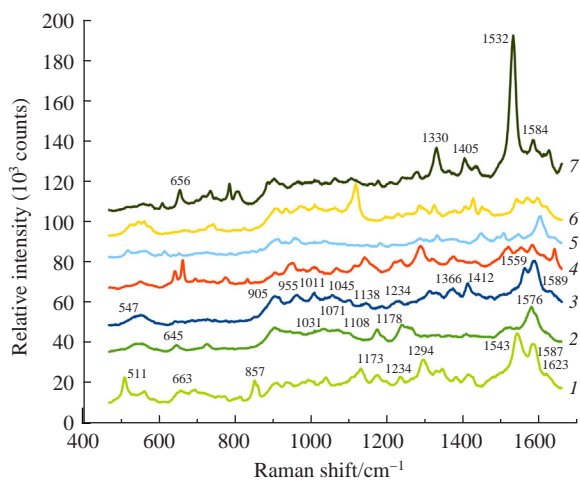


Figure 4 SERS measurements of 0.1 μM analytes with samples of nanostructured silver octahedra (series 3, 0.5 mg of PVP) using a combinatorial approach. Analytes and conditions: (1) *p*-benzoquinone,^{13,14} (2) thiophenol,^{13,14} (3) cysteamine,¹⁵ (4) *p*-benzoquinone with cysteamine-modified silver octahedra, (5) *p*-benzoquinone with thiophenol-modified silver octahedra, (6) silver octahedra co-modified with cysteamine and thiophenol and (7) *p*-benzoquinone with silver octahedra co-modified with cysteamine and thiophenol.

[¶] All measurements were performed using silver octahedra of series 3 (0.5 mg of PVP). Spectral Raman scattering and SERS data were analyzed using known data.^{11–17}

Cysteamine demonstrates amplification of a number of modes¹⁵ (Figure 4, spectrum 3) such as CH₂ scissoring (1589 cm^{-1}), NH₂ rocking and CH₂ wagging (1559 cm^{-1}), CH₂ rocking, NH₂ rocking and SH bending (1412 cm^{-1}), CH₂ wagging, NH₂ rocking and SH bending (1366 cm^{-1}), NH₂ rocking, CH₂ rocking and SH bending (1234 cm^{-1}), SH bending, CS bending, CH₂ twisting and CN stretching (1138 cm^{-1}), NH₂ twisting, CH₂ twisting and SH bending (1045 cm^{-1}), as well as SH bending, CC stretching and CN bending (955 cm^{-1}). Such a complexity of the observed modes indicates that this molecule can be considered as flexible and located on the silver surface due to the bond with the thiol group, most likely retaining a free amino group (terminating the surface layer).

The spectra of *p*-benzoquinone (Figure 4, spectrum 1) are complex and still controversial,¹⁷ as they contain many combinations of fundamental modes and overtones. In particular, the peak at 1543 cm^{-1} corresponds well to one of the overtones with the a_g symmetry (C–C stretching vibrations). This is mainly due to the presence of a conjugated system of C=C and C=O bonds and the interrelation of excited electronic states and vibration mode peculiarities.

The most interesting features of the SERS data are represented by the spectra of combinations of anchoring molecules modifying silver octahedra with those probe analyte molecules that are added (Figure 4, spectra 4–7). In particular, the co-modification of nanostructured silver with thiophenol and cysteamine (Figure 4, spectrum 6) gives almost nothing new; the resulting spectra are a combination of SERS from both modifying substances that cover the silver surface. The addition of *p*-benzoquinone to silver octahedra pre-modified with thiophenol (Figure 4, spectrum 5) leads to negligible changes in the spectral characteristics, which may mean that thiophenol almost completely covers the silver surface and does not form stable CTC with *p*-benzoquinone, thus remaining the only molecular type that generates SERS signal. At the same time, *p*-benzoquinone becomes visible by SERS if the silver octahedra are modified with cysteamine (Figure 4, spectrum 4). This would be possible if the hydrogen bonds of the ‘free’ amine groups of cysteamine, terminating the chemisorbed surface layer, attracted and held *p*-benzoquinone molecules on/near the surface of the silver octahedra and, thus, both substances contributed to SERS, while only a simple combination of spectra has so far been observed.

Finally, octahedral pseudomorphs of nanostructured silver, co-modified with amine and aryl-anchored groups, for example, cysteamine and thiophenol (see Figure 4, spectrum 6), drastically enhance some spectral modes upon the addition of *p*-benzoquinone (Figure 4, spectrum 7). In particular, the 1543 cm^{-1} mode of *p*-benzoquinone becomes highly intense, also showing a slight shift in its position. This is similar to previous observations¹⁸ that discussed that CTCs could provide additional amplification by SERS due to charge transfer and the involvement of electronic components in the resonant SERS. Apparently, a synergistic effect is observed here due to a combination of enhanced chemical sorption of quinone through the hydrogen bonds of the amino groups of cysteamine and charge transfer effects for quinone analytes and thiophenol located nearby. Thus, this new approach can be proposed as a suitable practical way to combinatorially modify the surface of SERS-active materials for the selective capture and detection of target analytes.

This work was supported by the Russian Science Foundation (grant no. 20-73-00257). The authors thank A. E. Baranchikov and V. K. Ivanov (IGIC RAS) and the Development program ‘The Future of the Planet and Global Environmental Changes’ of the Interdisciplinary Scientific and Educational School of M. V. Lomonosov Moscow State University. SEM studies were

carried out on the equipment of the Joint Research Center for Physical Methods of Research of N. S. Kurnakov Institute of General and Inorganic Chemistry of the Russian Academy of Sciences (JRC PMR IGIC RAS).

References

- 1 M. Moskovits, *Rev. Mod. Phys.*, 1985, **57**, 783.
- 2 R. A. Alvarez-Puebla and L. M. Liz-Marzán, *Small*, 2010, **6**, 604.
- 3 X. X. Han, R. S. Rodriguez, C. L. Haynes, Y. Ozaki and B. Zhao, *Nat. Rev. Methods Primers*, 2021, **1**, 87.
- 4 O. E. Eremina, A. A. Semenova, E. A. Sergeeva, N. A. Brazhe, G. V. Maksimov, T. N. Shekhovtsova, E. A. Goodilin and I. A. Veselova, *Russ. Chem. Rev.*, 2018, **87**, 741.
- 5 A. A. Semenova, A. P. Semenov, E. A. Gudilina, G. T. Sinyukova, N. A. Brazhe, G. V. Maksimov and E. A. Goodilin, *Mendeleev Commun.*, 2016, **26**, 177.
- 6 J. Fang, S. Liu and Z. Li, *Biomaterials*, 2011, **32**, 4877.
- 7 J. Henzie, M. Grünwald, A. Widmer-Cooper, P. L. Geissler and P. Yang, *Nat. Mater.*, 2012, **11**, 131.
- 8 A. A. Semenova, I. A. Veselova, N. A. Brazhe, A. V. Shevelkov and E. A. Goodilin, *Pure Appl. Chem.*, 2020, **92**, 1007.
- 9 A. A. Semenova, S. V. Savilov, A. E. Baranchikov, V. K. Ivanov and E. A. Goodilin, *Mendeleev Commun.*, 2019, **29**, 395.
- 10 J. Yang, L. Qi, C. Lu, J. Ma and H. Cheng, *Angew. Chem., Int. Ed.*, 2005, **44**, 598.
- 11 M. Del Pilar Rodríguez-Torres, L. A. Díaz-Torres and S. Romero-Servin, *Int. J. Mol. Sci.*, 2014, **15**, 19239.
- 12 N. Nuntawong, M. Horprathum, P. Eiamchai, K. Wong-ek, V. Patthanasettakul and P. Chindaudom, *Vacuum*, 2010, **84**, 1415.
- 13 F. Madzharova, Z. Heiner and J. Kneipp, *J. Phys. Chem. C*, 2020, **124**, 6233.
- 14 G. V. Pavan Kumar and C. Narayana, *Curr. Sci.*, 2007, **93**, 778.
- 15 A. Kudelski and W. Hill, *Langmuir*, 1999, **15**, 3162.
- 16 J. Makuraza, T. Pogrebnaya and A. Pogrebnoi, *Int. J. Mater. Sci. Appl.*, 2015, **4**, 314.
- 17 K. Palmö, L.-O. Pietilä, B. Mannfors, A. Karonen and F. Stenman, *J. Mol. Spectrosc.*, 1983, **100**, 368.
- 18 A. Sidorov, O. Vashkinskaya, A. Grigorieva, T. Shekhovtsova, I. Veselova and E. Goodilin, *Chem. Commun.*, 2014, **50**, 6468.

Received: 11th May 2022; Com. 22/6894